Desalination and Water Treatment
www.deswater.com

doi: 10.1080/19443994.2015.1014853

57 (2016) 6761–6771
March

Taylor & Francis
Taylor & Francis Group

Fenton oxidation of indole-3-acetic acid by iron alginate beads

S. Ben Hammouda, N. Adhoum, L. Monser*

Laboratoire de Chimie Analytique et d'Electrochimie, Institut National des Sciences Appliquées et de Technologie, University of Carthage, Centre Urbain Nord, B.P.No. 676, 1080 Tunis Cedex, Tunisia, Tel. +216 22 625196; Fax: +216 71 704329; emails: Samiabenhammouda@gmail.com (S. Ben Hammouda), nafaa.adhoum@gmail.com (N. Adhoum), lotfi.monser@insat.rnu.tn (L. Monser)

Received 3 March 2014; Accepted 22 January 2015

ABSTRACT

A heterogeneous Fenton reaction using Iron alginate beads (Fe-AB) was evaluated for the removal of an N-heterocyclic compound indole-3-acetic acid (IAA), which ranked as uremic toxin and an herbicide derivative. The efficiency of the process was studied as a function of the experimental conditions: initial pH; H_2O_2 dose, temperature, initial concentrations of IAA, and Iron alginate beads loading. Under the best experimental conditions: pH 3.0; H_2O_2 dose = 9.8 mM; and [alginate beads] = 1.0 g L^{-1}, it was possible to remove 100% of 0.11 mM IAA in 120 min in a batch reaction at 25˚C. The experimental results indicate also that the use of this catalyst allows a significant removal of total organic carbon without significant leaching of Fe ions. A kinetic analysis showed that the removal of IAA followed a first-order kinetics model. In addition, the Fe-AB catalyst can be reused for successive runs, without significant loss of activity.

Keywords: Alginate beads; *Indole-3-acetic* acid; Iron (II); Heterogeneous Fenton process

1. Introduction

Intensive use of herbicides in agriculture to improve the quality and quantity of production has led to a pervasive contamination problem. In fact, herbicides in soil may be taken up by plants, degraded into other chemical forms, or leached downward, possibly to groundwater and run off into surface waters with rainfall and/or irrigation. Therefore, the control and treatment of herbicides and their derivatives in water is one of the major measures in environmental protection [1–4].

The auxinic herbicides were among the first selective organic herbicides developed during the 1940s. They continue to be one of the most widespread and important herbicide families in use [5,6]. Among numerous compounds, indole-3-acetic acid (IAA), a nitrogen heterocyclic compound (NHC) (Fig. 1), also known as auxin, is a plant growth regulator and the major derivative of most auxin herbicides [7,8]. At high concentration, auxin stimulates the production of ethylene [9,10]. Excess ethylene can inhibit elongation growth, cause leaves to fall, and even kill the plant [11].

IAA is also ranked as a uremic toxin and can cause uremic syndrome. Uremic syndrome may affect any part of the body and can cause nausea, vomiting, loss of appetite, and weight loss. It can also cause changes in mental status, such as confusion, reduced awareness, agitation, psychosis, seizures, and coma.

---

*Corresponding author.

1944-3994/1944-3986

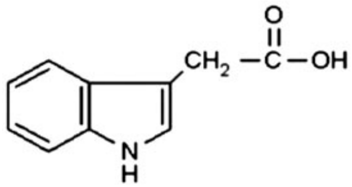

Fig. 1. Chemical structure of IAA.

Abnormal bleeding, such as bleeding spontaneously or profusely from a very minor injury, can also occur. Heart problems, such as an irregular heartbeat, inflammation in the sac that surrounds the heart, and increased pressure on the heart, can be seen in patients with uremic syndrome. Shortness of breath from fluid buildup in the space between the lungs and the chest wall (pleural effusion) can also be present. IAA may induce endothelial dysfunction, inflammation, and oxidative stress, leading to increased cardiovascular risk [12–16]. It can be found or may be developing in untreated wastewaters, depending on ambient conditions, and affect human health. Therefore, it is environmentally important to develop processes to remove it economically and effectively.

Advanced oxidation processes, and among them the Fenton processes, are particularly attractive and mainly used to destroy hazardous and refractory organic pollutants. Fenton process involves a catalytic reaction (Eq. (1)) between hydrogen peroxide and ferrous ion in an acidic aqueous solution to produce hydroxyl radicals ($^{\cdot}OH$), a non-selective chemical oxidant with high oxidation potential E° ($OH^{\cdot}/H_2O$) = 2.8 V/NHE (*normal hydrogen electrode*) [17,18]. The mechanism of Fenton reaction is presented as follows [19]:

$$Fe^{2+} + H_2O_2 \rightarrow Fe^{3+} + OH^- + OH^{\cdot} \quad (1)$$

$$Fe^{3+} + H_2O_2 \rightarrow Fe^{2+} + HO_2^{\cdot} + H^+ \quad (2)$$

Nevertheless, the removal of sludge containing ferrous ion at the end of wastewater treatment by homogeneous Fenton process is costly and requires more complex post-treatments [20].

Recently, increasing attention is being paid to the heterogeneous catalysis by the immobilization of iron on different support materials in order to avoid the sludge separation step typical of the conventional homogeneous process [21–30].

Alginate has attracted researchers' attention as a natural chelating agent of chemical catalysts, and it has been reported that incorporating iron with alginate in bead form allows an easy separation and recovery of the catalyst from the treated water. Alginate is a natural polysaccharide extracted from brown algae, and it is very useful as it is cheap, non-toxic, and its production does not require high pressure or toxic organic solvents [31].

This study focuses on the applicability of Fe-AB as a heterogeneous Fenton catalyst in the degradation of an N-heterocyclic compound, IAA. The influence of various parameters such as initial reaction pH, temperature, H_2O_2 concentration, IAA concentration, and catalyst amount was investigated. The stability of alginate beads as an immobilizing support for iron was also evaluated. Finally, to assess the practicality of this catalyst in water treatment, we present our attempts to recover and reuse these beads several times.

2. Material and methods

2.1. Chemicals

All chemicals used were of analytical grade and used without further purification. Sodium alginate was purchased from Sigma (Spain). Hydrogen peroxide (30%) was obtained from Scharlau (France). IAA, ferrous sulfate heptahydrate, calcium chloride, sodium chloride, and sulfuric acid were all purchased from Prolabo (France). NaOH and H_2SO_4 solutions were applied for pH adjustment.

2.2. Preparation of catalysts (Fe-AB)

Sodium alginate solution (4.0% w/v) was prepared by dissolving an appropriate amount of alginic acid sodium salt in distilled water and then was dropped into a hardening solution composed of 0.1 mol L^{-1} Ca^{2+} ($CaCl_2 \cdot 2H_2O$) and 0.05 mol L^{-1} Fe^{2+} ($FeSO_4 \cdot 6H_2O$). A syringe needle was used to produce the spherical iron cross-linked calcium alginate beads (Fe-AB) at a dropping rate of approximate 1.0 mL min^{-1}. The formed particles (Fig. 2) were kept 2 h in the gelling solution, filtered off, washed with hydrochloric acid (10^{-3} mol L^{-1}), and repeatedly rinsed with distilled water before being dried in oven for 12 h at 50°C [31].

Cross-linked Ca-alginate beads (Ca-AB) were obtained by dropping a 4.0% sodium alginate into a 0.1 mol L^{-1} calcium chloride solution.

2.3. Experimental procedure

2.3.1. Degradation experiments

Both oxidation (without beads) and catalytic oxidation experiments were carried out in stoppered conical

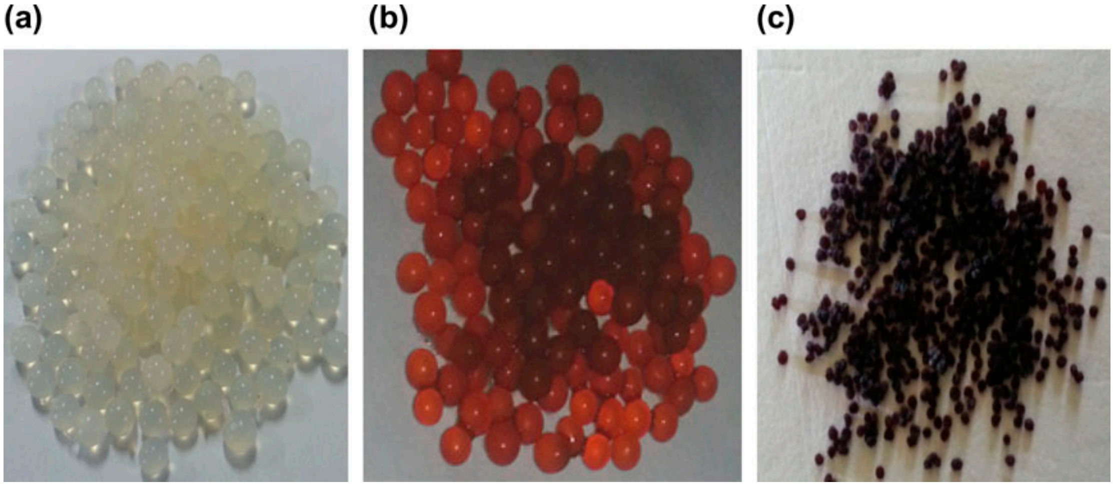

Fig. 2. Digital photographs of the prepared alginate beads at different physical state: (a) raw beads without iron, (b) raw beads containing iron, and (c) dried beads containing iron.

flasks containing different concentrations of IAA solutions (10–30 mol L^{-1}). The pH value of reactant solution was adjusted with 1.0 mol L^{-1} H_2SO_4 or NaOH solution. After the correction of pH to the selected value, the Fe-ABs catalysts (0–75 mg) were put into 50 mL of the aqueous IAA solution under continuous stirring, and then the required amount of hydrogen peroxide (0–98 mM) was added to start the reaction. Samples were withdrawn at selected time intervals and *analyzed at 278 nm using* a spectrophotometer *(BeckMan DU640B)*. The mineralization degree of IAA was measured from the total organic carbon (TOC) concentration changes using *Analytik jena TOC multi N/C* 2100 *analyzer*. All measurements were evaluated using standard deviations with the help of EURACHEM method uncertainty.

2.3.2. Adsorption test

Batch adsorption experiments were performed without H_2O_2 addition by varying the type (Ca-AB or Fe-AB) of beads. 50 mg of dry alginate beads was suspended into 50 mL of 20 mol L^{-1} IAA aqueous solution and then mixed by shaking at a temperature of 25℃ and pH 3.0 for the appropriate time. The adsorption was monitored by UV–visible spectroscopy (Beckman DU640B) at 278 nm.

3. Results and discussion

In an attempt to evaluate the predominate factor in pollutant destruction in Fe-AB process, the contribution of alginate adsorption and H_2O_2 oxidation was initially investigated. The efficiency of the process was studied as a function of the following experimental conditions: initial pH, H_2O_2 dose, temperature, initial concentrations of IAA, and Iron alginate beads loading.

3.1. Adsorptive removal of IAA

As reported in the literature, alginate beads can be used as an efficient adsorbent in wastewater treatment [30] mainly for the removal of heavy metal [32–36] and dyes [37,38]. In an attempt to discriminate between the contribution of alginate beads matrix to the adsorption phenomena or to catalytic oxidation processes, adsorption assays were initially carried out, at pH 3.0, using 20 mg L^{-1} of IAA, without H_2O_2 addition. As shown in Fig. 3, the concentration of IAA did not obviously decrease in the presence of Ca-AB alone. The IAA removal was also negligible in the presence of the supported Fe-AB catalyst. This finding of alginate sorption is similar to that found by

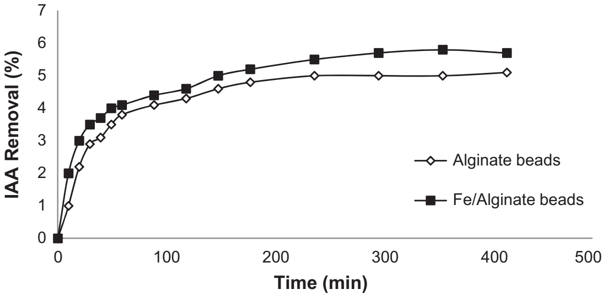

Fig. 3. Adsorption kinetics of IAA onto AB and Fe-AB. Experimental conditions: pH 3.0, amount of AB = 1.0 g L^{-1}, and [IAA] = 0.11 mM.

Bezbaruah et al. [39], indicating that IAA hardly adsorbed on the Fe-ABs surface.

3.2. Oxidative removal of IAA by hydrogen peroxide

It is known that hydrogen peroxide is a powerful oxidant and it can be used as an oxidizing agent to destroy many water pollutants. Therefore, before applying the Fenton process, it is primordial to study the effect of H_2O_2 alone (without addition of Fe-AB catalysts) on IAA degradation using a solution contains 0.11 mM of IAA at pH 3.0 and without addition of Fe-AB catalyst.

Fig. 4 represents the effect of H_2O_2 dose on the removal of 0.11 mM IAA. It appears that efficiency of hydrogen peroxide alone is negligible and the maximum IAA removal after 240 min was only 7%. There is an increase in the removal efficiency with an increase in the dose. However, that increase is just marginal.

Similar findings have been reported from other studies [40–45]. This result can be ascribed to the weaker oxidation potential of peroxide hydrogen (H_2O_2) than those of hydroxyl radicals ($OH^{\cdot}$) and perhydroxyl radicals ($HO_2^{\cdot}$).

The performance of H_2O_2 as an oxidant can be enhanced by generating highly activated species ($OH^{\cdot}$) by adding catalyst to the effluent.

3.3. Fenton process

The effects of main operational parameters, such as the initial pH, the temperature, the concentration of hydrogen peroxide, and the amount of catalyst, were investigated and optimized, as they may significantly affect the catalytic performance of the Iron alginate beads.

3.3.1. Effect of hydrogen peroxide concentration

Hydrogen peroxide was the basis for the radical generation in Fenton's oxidation process. The hydroxyl radicals ($OH^{\cdot}$), produced from the reaction between H_2O_2 and Fe^{2+}, either oxidize the pollutant and other intermediates, or react with the oxidant itself to cause reduction in pollutant removal efficiency. Initially, it can be expected that as the molar ratio of H_2O_2 to pollutant is increased, more $HO^{\cdot}$ radicals are available to attack the organic structure, and therefore, the degradation efficiency should increase.

Hence, an investigation of H_2O_2 consumption and optimization in Fenton's oxidation process was vital. The optimization of hydrogen peroxide concentration was carried out by varying H_2O_2 concentration from 0.98 to 9.8 mM and fixing the amount of Fe-AB to 1.0 g L^{-1} and the pH to 3.0. The effect of the amount of H_2O_2 addition on the removal of IAA was shown in Fig. 5. This figure shows an increase on the removal efficiency of IAA with increasing H_2O_2 concentration and increasing time. The increase was almost linear in the first 60 min and then steadily decreased to become almost constant. The linear increase at a H_2O_2 concentration from 0.98 to 4.9 mM was accompanied by an increased the removal efficiency of IAA from 8 to 50% in 60 min. It was shown that IAA degradation increased gradually with H_2O_2 concentration and complete degradation of IAA was achieved within 120 min in the presence of 9.8 mM H_2O_2 at pH 3.0, which is close to the optimum pH for Fenton's reaction (pH of 2.8). This is expected, since the production of the highly reactive $^{\cdot}OH$ produced by the catalytic decomposition of H_2O_2 was significantly accelerated by increasing H_2O_2 concentration as well as propagation reactions that form transient oxygen reactive species that aid in the destruction of organic pollutant [29].

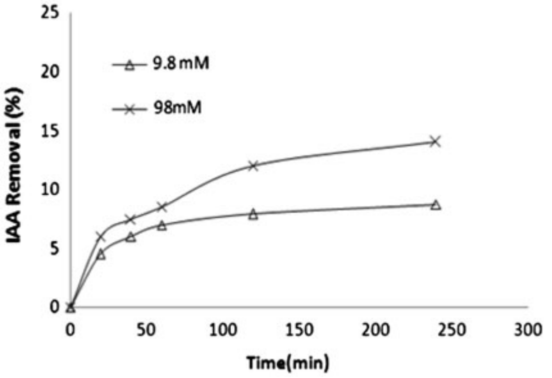

Fig. 4. Effect of H_2O_2 alone on the degradation of IAA at 0.11 mmol L^{-1} IAA and pH 3.0.

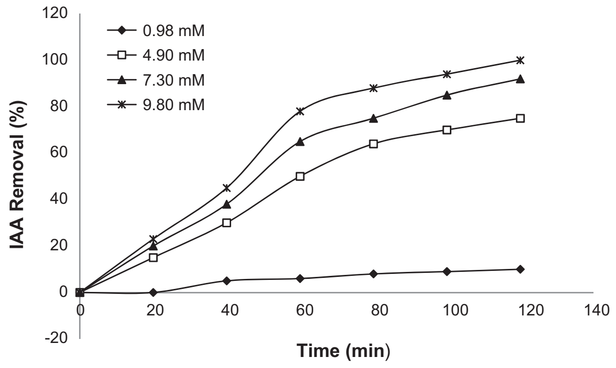

Fig. 5. Effect of hydrogen peroxide concentration on IAA removal efficiency at 0.11 mmol L^{-1} IAA, 298 K, initial pH 3.0, and 1.0 g L^{-1} Fe-AB.

3.3.2. *Effect of catalyst concentration*

In order to assess the effect of Iron alginate beads loading, a series of experiments were carried out in which the amount of catalyst was changed from 0.25 to 1.5 g L^{-1} (0.01–0.075 g) and all other operational parameters were kept constant. As shown in Fig. 6, within 120 min, the removal efficiency of IAA increased from about 10 to 100% when Fe-AB loading was increased from 0.25 to 1 g L^{-1}. These results could be explained by the fact that the increase in the amount of catalyst will supply more active iron sites that will accelerate the decomposition of H_2O_2 which in turn significantly increases the number of hydroxyl radical.

However, a significant improvement was not seen for an amount of Iron alginate beads higher than 1 g L^{-1}. Therefore, the optimum catalyst loading was fixed at 1 g L^{-1} for all subsequent runs, as it gave the highest efficiency.

3.3.3. *Effect of solution initial pH*

The efficacy of the Fenton reactions depends on the pH; therefore, its impact on the catalytic activity of Iron alginate beads was studied for IAA degradation. For this purpose, the experiments were carried out at initial pH values that varied from 2 to 11, without any modifications or control of the pH during the process. The obtained results (Fig. 7) show that the maximum removal capacity of IAA was observed at pH 3.0.

Above this pH, the removal efficiency of IAA rapidly decreased with the increase in pH. Above pH 7, the destruction of IAA scarcely occurred. In fact, H_2O_2 is unstable in basic solutions and may decompose to give oxygen and water, losing some of its oxidation ability. However, at pH 2, the reaction of H_2O_2 with Fe^{2+} (Eq. (3)) is seriously affected causing the reduction in $OH^{\cdot}$ radical production due to $OH^{\cdot}$ scavenging by H^+ ions according to Eq. (4), which explains the decrease of the removal efficiency at pH 2.

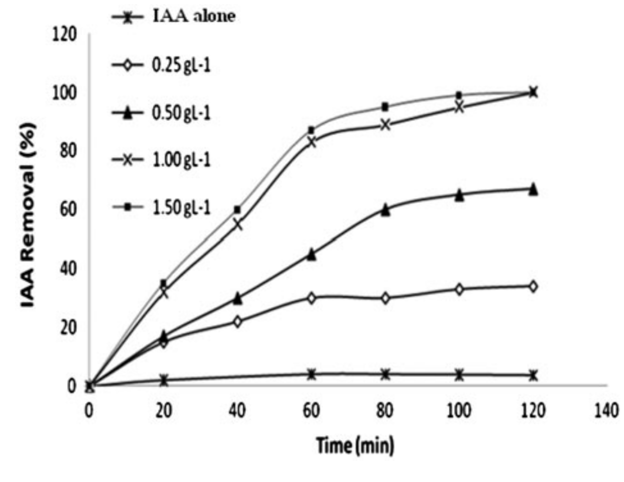

Fig. 6. The influence of alginate concentration on IAA removal efficiency at 0.11 mM IAA, initial pH 3.0, and 9.8 mM H_2O_2.

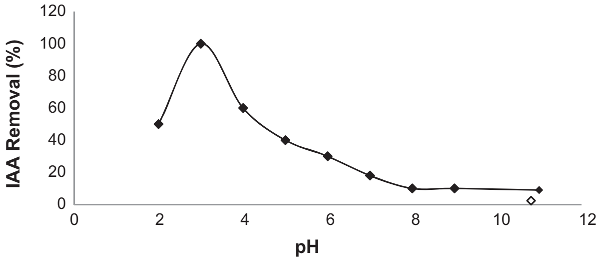

Fig. 7. Effect of pH on IAA degradation by Fenton's oxidation at 0.11 mM IAA, 9.8 mM H_2O_2, 1.0 g L^{-1} Fe-AB.

$$Fe^{2+} + H_2O_2 \rightarrow Fe^{3+} + OH^- + OH^{\cdot} \quad (3)$$

$$OH^{\cdot} + H^+ + e^- \rightarrow H_2O \quad (4)$$

3.3.4. *Effect of IAA initial concentration*

In wastewater treatment plants, the pollutant concentration present in the effluent is usually variable. From an application point of view, it is important to study the dependence of removal efficiency on the initial concentration of the contaminant and to determine the maximum amount that would be destroyed with a

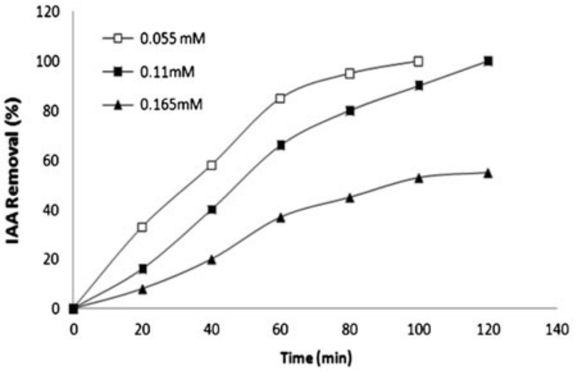

Fig. 8. Effect of IAA initial concentration on the removal efficiencyat 9.8 mM H_2O_2, pH 3, and 1.0 g L^{-1} Fe-AB.

fixed reagent concentration. Thus, the effect of IAA concentration on the degradation efficiency was investigated in the concentration range that varied between 0.055 and 0.165 mM. As seen in Fig. 8, it can be noted that the removal rate increased with the decrease of initial concentration of IAA. After a period of 90 mins a removal of 100, 85 and 55% was, respectively, achieved with 0.055, 0.11, and 0.165 mM of IAA.

These results could be attributed to the fact that an increase in IAA initial concentration leads to an increase in the number of pollutant molecules. Knowing that H_2O_2 concentration and the catalyst amount were maintained constant, the hydroxyl radical concentration remains also constant and is not enough to degrade all IAA molecules.

3.3.5. Effect of temperature

Different temperatures were investigated in order to evaluate the role of temperature in Fenton process. Moderating the temperature is necessary not only for economic reasons, but also for safety reasons as well. For this purpose, temperatures in the range 25–50˚C were selected considering environmental conditions located in Tunisia. Experiments were carried out at IAA concentration of 0.11 mM, H_2O_2 concentration of 9.8 mM, and Fe-AB concentration of 1.0 g L^{-1}.

As shown in Fig. 9, the increase on the temperature has a positive impact on the degradation of IAA. A significant enhancement of the degradation was produced when the temperature was increased from 25 to 55˚C. This is due to the fact that higher temperature increased the reaction rate between hydrogen peroxide and Fe-AB catalyst, thus increasing the rate of production of $OH^{\cdot}$ radical. In addition, higher temperature can provide more energy for the reactant molecules to overcome reaction activation energy [46].

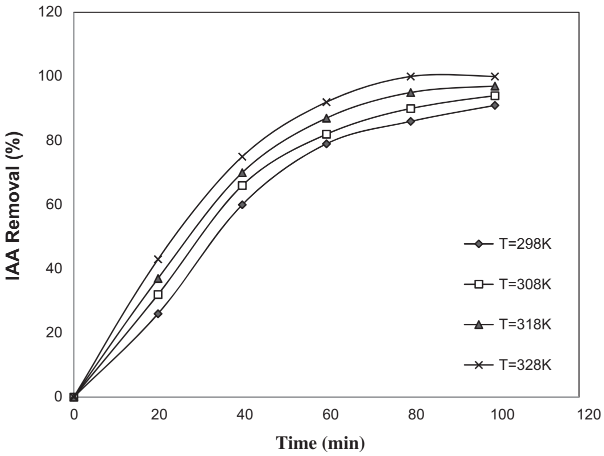

Fig. 9. The influence of temperature on IAA removal efficiency at pH 3.0, 0.11 mM IAA, 9.8 mM H_2O_2, and 1.0 g L^{-1} Fe-AB.

3.3.6. Kinetic of the heterogeneous Fenton reaction

In order to determine the oxidation kinetics of IAA by Fenton process, the kinetic parameters were studied. Statistically the regression of the data was conducted for zero-, first- and second-order kinetic [47].

Results obtained (Table 1) show that first order kinetic models provided better R^2 values than the zero- and second-order kinetic models. Kinetic plots are illustrated in Fig. 10.

The apparent kinetic constant obtained by linear regression analysis are 2.26×10^{-2}, 2.82×10^{-2}, 3.40×10^{-2}, and 4.37×10^{-2} min^{-1} for the temperature of 25, 35, 45, and 55˚C, respectively. Kinetic constants increased approximately two times as the temperature increased from 25 to 55˚C.

From the kinetic data at different temperatures, it was possible to determine the initial rates of reaction and then calculate the apparent activation energy by applying the Arrhenius equation [48].

$$K = A \exp\left(-E_a/RT\right) \tag{5}$$

where K is the rate constant which controls process, A is the Arrhenius constant, T is the solution temperature (K), E_a is the apparent activation energy (kJ mol^{-1}), and R is the ideal gas constant (0.0083 kJ mol^{-1} K^{-1}).

From the corresponding Arrhenius-type plot (Fig. 11), values of A and E_a can be calculated as 38.91 and 26.99 kJ mol^{-1}, respectively. Temperature and kinetic constant are highly correlated ($R^2 = 0.99$).

Typical thermal reactions usually have reaction activation energies between 60 and 250 kJ mol^{-1} [49,50]. The apparent activation energy in this study implied that the degradation of IAA in aqueous solution by the heterogeneous Fenton oxidation process required much lower activation energy which

Table 1
R^2 values at different temperature

	Temperature			
Type of kinetic	25˚C	35˚C	45˚C	55˚C
Zero order	0.9191	0.8632	0.846	0.7993
First order	0.9861	0.989	0.9823	0.9943
Second order	0.7905	0.7739	0.7954	0.9230

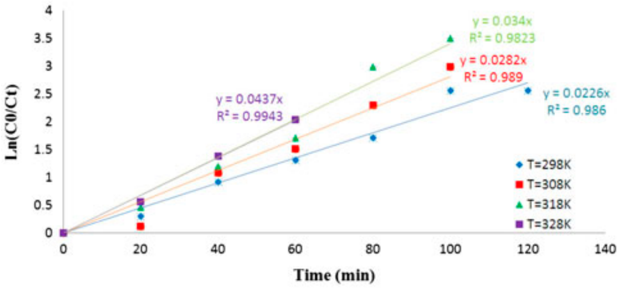

Fig. 10. First-order kinetic plots for different temperature.

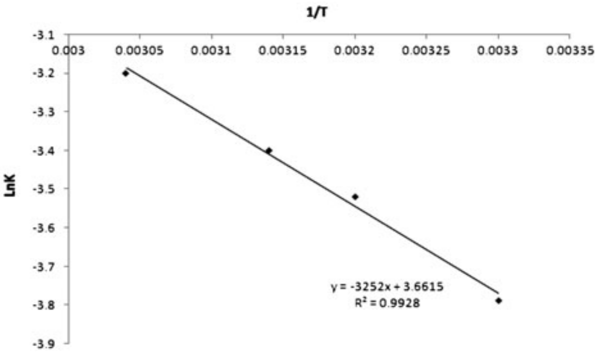

Fig. 11. Arrhenius-typeplot of the apparent first-order kinetic constants.

indicates that the oxidative reaction proceeds with low energy barrier and could be easily achieved.

3.3.7. IAA mineralization and evolution of degradation intermediates

It is known that the oxidation of organic compounds is accompanied by the formation of reaction intermediates and some of them could be long-lived and even more toxic than their parent compounds [51,52]. Efficient mineralization of the pollutant during the degradation is essential for avoiding secondary pollution in practical applications. Therefore, it is necessary to measure the mineralization degree of the IAA to evaluate the degradation level applied by the Fenton process. The concentration of TOC was selected as a mineralization index of the IAA destruction [53,54]. After contact time for 4 h (Fig. 12), 100% of the TOC was eliminated, indicating that IAA was effectively mineralized in this process. Furthermore, and in an attempt to identify the intermediates formed during the degradation process, high-performance liquid chromatography with diode array detection was used. Chromatograms (Fig. 13) of samples

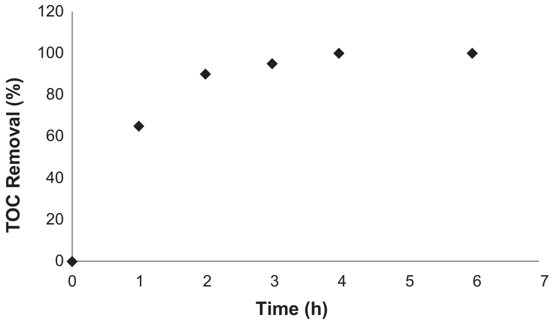

Fig. 12. TOC removal of IAA by Fenton process at 9.8 mM H_2O_2, 0.11 mM IAA, 1.0 g L^{-1} Fe-AB, and pH 3.0.

collected at selected time intervals during the treatment of 0.11 mM IAA showed a gradual disappearance of IAA peak ($t_R = 6.7$ min). The disappearance of IAA peak was accompanied by the appearance of new peaks that elute before the parent compound, which could be attributed to oxidation intermediates.

As shown in Fig. 13, after 120 min, the degradation of IAA resulted in a complete disappearance of IAA and the appearance of two major peaks (corresponding to carboxylic acid or/and intermediates products) at the following retention times: peak 1 at 3.6 min and peak 2 at 4.1 min.

The final analysis of samples after 4 h of treatment indicated the complete removal of any compound. These results mean that intermediates are eventually degraded into CO_2 and H_2O.

3.3.8. Stability and catalyst re-use test

Successive tests were performed in order to assess the stability of Iron alginate beads (Fe-AB) as heterogeneous Fenton catalysts for removal of IAA and thus to observe the possibility of catalyst reuse. It should be noted that Fe-alginate gel beads were produced by the reaction of alginate with Fe^{2+} ions in aqueous solution; therefore, their diameter and Fe content were affected significantly by the concentration of alginate or $FeSO_4$ solution used. Sodium alginate solution with higher concentration than 4.0 wt.% showed too high viscosity to be used for the preparation of uniform Fe-alginate gel beads.

3.3.9. Stability test

Leaching of iron from alginate can occur during the oxidation process and thus generate a secondary pollution. In order to evaluate the stability of the *heterogeneous catalyst*, the amount of iron released into solution during the oxidation process was analyzed.

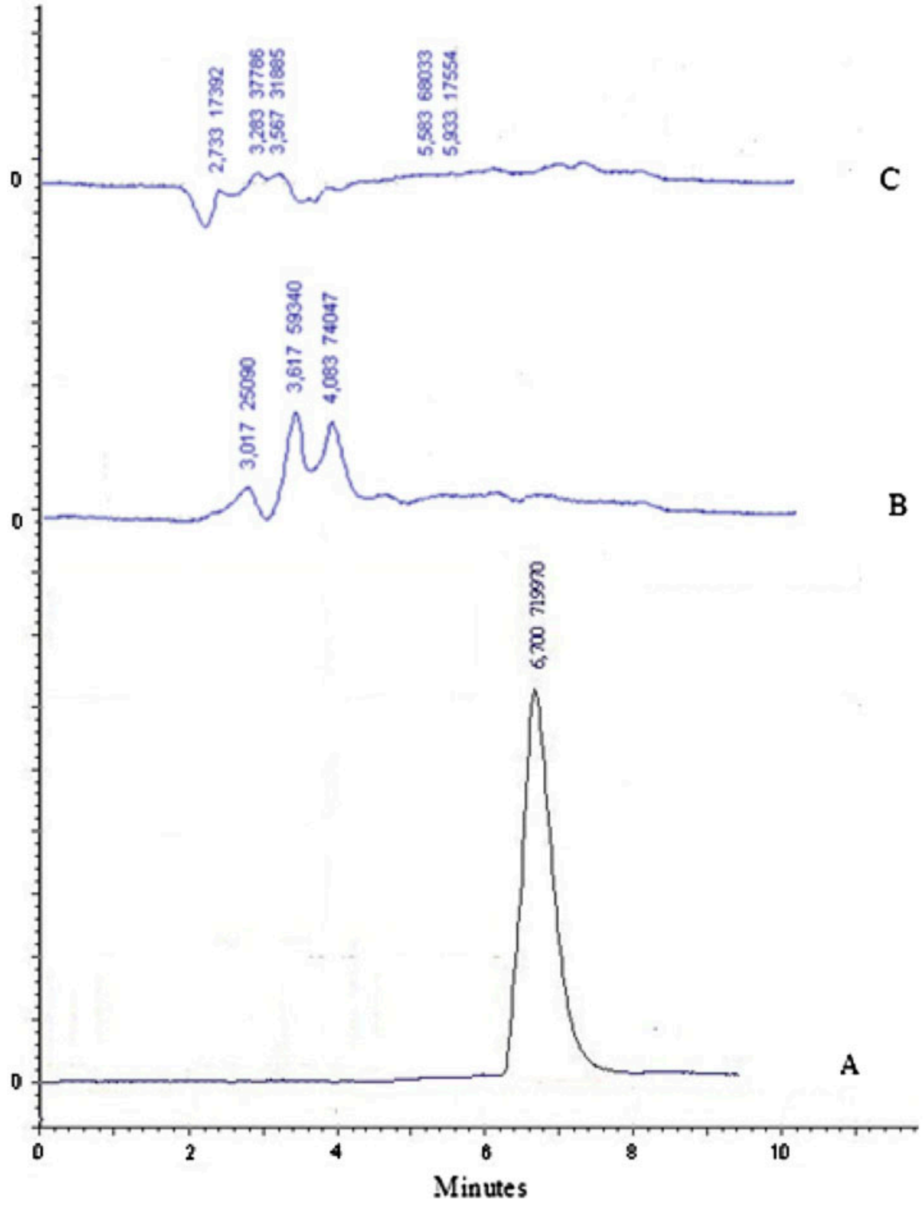

Fig. 13. Time evolution of IAA and aromatic intermediates generated during treatment; 0.11 mM IAA, initial pH 3.0, 9.8 mM H_2O_2, and 1.0 g L^{-1} Fe-AB. Chromatographic conditions: *Column C18*, mobile phase containing methanol:water (80:20 v/ v) at a flow rate of 1 mL min^{-1}. (A) Before treatment, (B) after 2 h of treatment, and (C) after 4 h of treatment.

Results showed that the amount of iron leached into solution is very low (does not exceed 0.6 mol L^{-1}). Therefore, Iron alginate beads are sufficiently stable to be used without causing metal pollution problems.

In order to check if the amounts of leached iron are responsible for the catalytic activity and to evaluate the contribution of the homogeneous reaction during the heterogeneous Fenton process, a trial was carried out using a solution containing iron ions (0.6 mol L^{-1}). The concentration of IAA and H_2O_2 was similar to concentration used for the heterogeneous experiment. The results (Fig. 14) demonstrate that the catalytic activity of the fraction of iron leached from Iron alginate beads is negligible. Therefore, the contribution of the homogeneous reaction during the heterogeneous Fenton process could be neglected.

3.3.10. Catalyst re-use test

In an attempt to evaluate the stability and reuse of Fe-AB, four consecutive essays were repeated using the same amount of Fe-AB previously used. After each

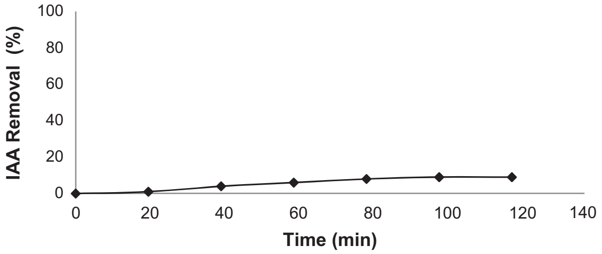

Fig. 14. Catalytic activity of the fraction of iron leached during the heterogeneous treatment at 0.11 mM IAA, initial pH 3.0, 9.8 mM H_2O_2, and $[Fe^{2+}] = 0.6$ mol L^{-1}.

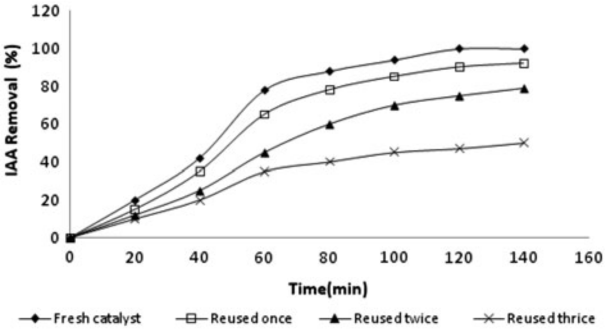

Fig. 15. Conversion of IAA as a function of the time of reaction in different conditions at 0.11 mM IAA, initial pH 3.0, and 9.8 mM H_2O_2.

cycle, the catalyst was removed by filtration, thoroughly washed with distilled water, and followed by drying at 50˚C for 4 h. A comparative study between fresh and reused catalyst is depicted in Fig. 15. As it can be observed, the catalytic activity of Iron alginate beads decreased after successive runs. The loss of activity shown at the forth cycle could be attributed to cumulative leaching of iron species from catalyst support after three successive uses.

The Iron alginate beads catalyst still showed good stability for the degradation of IAA after three recycles, but in the forth re-use cycle, a full dissociation of the catalyst was observed after one hour of treatment.

4. Conclusions

The results showed that the Fe-AB heterogeneous Fenton process is an efficient and economic method for the removal of IAA, provided that the catalyst and hydrogen peroxide are present in suitable concentrations. The degradation efficiencies were influenced by the initial concentration of IAA, the pH of solution, the temperature and the amount of hydrogen peroxide and catalyst.

The optimum conditions for the degradation of IAA were observed at pH 3.0, with an Fe^{2+}-alginate beads concentration of 1.0 g L^{-1} and initial H_2O_2 concentration of 9.8 mM with a pollutant concentration of 0.11 mM. After 120 min, the catalyst allows the total elimination of IAA and a significant TOC removal, without generating additional pollution by iron hydroxide sludge. In addition, the catalyst can be reused for successive runs, without significant loss of activity. IAA degradation follows a first-order kinetics, and the apparent activation energy of the reaction was calculated to be 26.99 kJ mol^{-1}. In view of the foregoing discussion, the developed catalyst would be of potential application, as it offers interesting assets such as simplicity, low cost, good structural stability, easy recovery, and stable catalytic activity in repetitive reaction cycle.

References

[1] E. Ovidi, G. Gambellini, A.R. Taddei, G. Cai, C.D. Casino, M. Ceci, S. Rondini, A. Tiezzi, Herbicides and the microtubular apparatus of *Nicotiana tabacum* pollen tube: Immunofluorescence and immunogold labelling studies, Toxicol. in Vitro 15 (2001) 143–151.

[2] M. Pateiro-Moure, M. Arias-Estévez, E. López-Periago, E. Martínez-Carballo, J. Simal-Gándara, Occurrence and downslope mobilization of quaternary herbicide residues in vineyard-devoted soils, Bull. Environ. Contam. Toxicol. 80 (2008) 407–411.

[3] J.J. Zhang, Y.C. Lu, J.J. Zhang, L.R. Tan, H. Yang, Accumulation and toxicological response of atrazine in rice crops, Ecotoxicol. Environ. Saf. 102 (2014) 105–112.

[4] D.M. Silburn, J.L. Foley, R.C. deVoil, Managing runoff of herbicides under rainfall and furrow irrigation with wheel traffic and banded spraying, Agric. Ecosyst. Environ. 180 (2013) 40–53.

[5] J. Mithila, J.C. Hall, Transfer of auxinic herbicide resistance from *Brassica kaber* to *Brassica juncea* and *Brassica rapa* through embryo rescue, In Vitro Cell. Dev. Biol. Plant 49 (2013) 461–467.

[6] H.G. Zheng, J.C. Hall, Understanding auxinic herbicide resistance in wild mustard: Physiological, biochemical, and molecular genetic approaches, Weed Sci. 49 (2001) 276–281.

[7] M. Qamar, M. Muneer, Comparative photocatalytic study of two selected pesticide derivatives, indole-3-acetic acid and indole-3-butyric acid in aqueous suspensions of titanium dioxide, J. Hazard. Mater. 120 (2005) 19–27.

[8] E. Sait Kurter, A. K. Ayan, Effects of gibberellic acid (GA3) and indole-3-acedic acid IAA on flowering, stalk elongation and bulb characteristics of tulip (*Tulipa gesneriana* Var. Cassini), Pak. J. Biol. Sci. 8 (2005) 273–277.

[9] S. Spaepen, J. Vanderleyden, R. Remans, Indole-3-acetic acid in microbial and microorganism-plant signaling, FEMS Microbiol. Rev. 31 (2007) 425–448.

[10] S.P. Burg, E.A. Burg, Ethylene formation in pea seedlings; its relation to the inhibition of bud growth caused by indole-3-acetic acid, Plant Physiol. 7 (1968) 1069–1074.

[11] R. Maor, S. Haskin, H.L. Kedmi, A. Sharon, In planta production of indole-3-acetic acid by *Colletotrichum gloeosporioides* f. sp. *Aeschynomene*, Appl. Environ. Microbiol. 70 (2004) 1852–1854.

[12] L. Dou, M. Sallée, C. Cerini, S. Poitevin, B. Gondouin, N. Jourde-Chiche, K. Fallague, P. Brunet, R. Calaf, B. Dussol, B. Mallet, F. Dignat-George, S. Burtey, The cardiovascular effect of the uremic solute indole-3 acetic acid, J. Am. Soc. Nephrol. 26 (in press), doi: 10.1681/ASN.2013121283.

[13] M. Satoh, H. Hayashi, M. Watanabe, K. Ueda, H. Yamato, T. Yoshioka, M. Motojima, Uremic toxins overload accelerates renal damage in a rat model of chronic renal failure, Nephron Exp. Nephrol. 95 (2003) 111–118.

[14] B. Gondouin, C. Cerini, L. Dou, M. Sallée, A. Duval-Sabatier, A. Pletinck, R. Calaf, R. Lacroix, N. Jourde-Chiche, S. Poitevin, L. Arnaud, R. Vanholder, P. Brunet, F. Dignat-George, S. Burtey, Indolic uremic solutes increase tissue factor production in endothelial cells by the aryl hydrocarbon receptor pathway, Kidney Int. 84 (2013) 733–744.

[15] H.A.M. Mutsaers, M.J.G. Wilmer, D. Reijnders, J. Jansen, P.H.H. van den Broek, M. Forkink, E. Schepers, G. Glorieux, R. Vanholder, L.P. van den Heuvel, J.G. Hoenderop, R. Masereeuw, Uremic toxins inhibit renal metabolic capacity through interference with glucuronidation and mitochondrial respiration, BBA-Acta, Mol. Basis Dis. 1832 (2013) 142–150.

[16] R. Calaf, C. Cerini, C. Génovésio, P. Verhaeghe, N. Jourde-Chiche, D. Bergé-Lefranc, B. Gondouin, L. Dou, S. Morange, A. Argilés, P. Rathelot, F. Dignat-George, P. Brunet, P. Charpiot, Determination of uremic solutes in biological fluids of chronic kidney disease patients by HPLC assay, J. Chromatogr. B Anal. Technol. Biomed. Life Sci. 897 (2011) 2281–2286.

[17] S. Contreras, M.S. Yalfani, F. Medina, J.E. Sueiras, Effect of support and second metal in catalytic in-situ generation of hydrogen peroxide by Pd-supported catalysts: Application in the removal of organic pollutants by means of the Fenton, Appl. Catal., B 89 (2009) 519–526.

[18] J.A. Zazo, J.A. Casas, C.B. Molina, A. Quintanilla, J.J. Rodriguez, Evolution of ecotoxicity upon Fenton's oxidation of phenol in water, Environ. Sci. Technol. 41 (2007) 7164–7170.

[19] G.E. Ustuna, S.K. Akal Solmaza, T. Morsunbula, H.S. Azakb, Advanced oxidation and mineralization of 3-indole butyric acid (IBA) by Fenton and Fenton-like processes, J. Hazard. Mater. 180 (2010) 508–513.

[20] N. Dulova, M. Trapido, A. Dulov, Catalytic degradation of picric acid by heterogeneous Fenton-based processes, Environ. Technol. 32 (2011) 439–446.

[21] T. Liu, H. You, Q. Chen, Heterogeneous photo-Fenton degradation of polyacrylamide in aqueous solution over Fe(III)–SiO_2 catalyst, J. Hazard. Mater. 162 (2009) 860–865.

[22] S. Barreca, J.J.V. Colmenares, A. Pace, S. Orecchio, C. Pulgarin, Neutral solar photo-Fenton degradation of 4-nitrophenol on iron-enriched hybrid montmorillonite-alginate beads (Fe-MABs), J. Photochem. Photobiol. A 282 (2014) 33–40.

[23] M. Bayat, M. Sohrabi, S.J. Royaee, Degradation of phenol by heterogeneous Fenton reaction using Fe/clinoptilolite, J. Ind. Eng. Chem. 18 (2012) 957–962.

[24] J. Herney-Ramirez, M.A. Vicente, L.M. Madeira, Heterogeneous photo-Fenton oxidation with pillared clay-based catalysts for wastewater treatment: A review, Appl. Catal. B 98 (2010) 10–26.

[25] Y. Dong, W. Dong, Y. Cao, Z. Han, Z. Ding, Preparation and catalytic activity of Fe alginate gel beads for oxidative degradation of azo dyes under visible light irradiation, Catal. Today 175 (2011) 346–355.

[26] I. Muthuve, B. Krishnakumar, M. Swaminathan, Novel Fe encapsulated mont morillonite K10 clay for photo-Fenton mineralization of Acid Yellow 17, Indian J. Chem. 51 (2012) 800–806.

[27] O. Iglesias, J. Gómez, M. Pazos, M.Á. Sanromán, Fenton oxidation of imidacloprid by Fe alginate gel beads, Appl. Catal., B 144 (2014) 416–424.

[28] Q. Huang, X. Shi, R. Pinto, E. Petersen, W. Weber, Tunable synthesis and immobilization of zero-valent iron nanoparticles for environmental applications, Environ. Sci. Technol. 42 (2008) 8884–8889.

[29] A. Dhaouadi, N. Adhoum, Heterogeneous catalytic wet peroxide oxidation of paraquat in the presence of modified activated carbon, Appl. Catal., B 97 (2010) 227–235.

[30] S. Sabhi, J. Kiwi, Degradation of 2,4-dichlorophenol by immobilized iron catalysts, Water. Res. 35 (2001) 1994–2002.

[31] E. Rosales, O. Iglesias, M. Pazos, M. Sanromán, Decolourisation of dyes under electro-Fenton process using Fe alginate gel beads, J. Hazard. Mater. 213–214 (2012) 369–377.

[32] S. Barreca, S. Orecchio, A. Pace, The effect of montmorillonite clay in alginate gel beads for polychlorinated biphenyl adsorption: Isothermal and kinetic studies, Appl. Clay Sci. 99 (2014) 220–228.

[33] Y. Ling Lai, M. Thirumavalavan, J. Fwu Lee, Effective adsorption of heavy metal ions (Cu^{2+}, Pb^{2+}, Zn^{2+}) from aqueous solution by immobilization of adsorbents on Ca-alginate beads, Toxicol. Environ. Chem. 92 (2010) 697–705.

[34] T. Dewangan, A. Tiwari, A.K. Bajpai Removal of cobalt ions from aqueous solution by adsorption onto cross-linked calcium alginate beads, J. Dispersion Sci. Technol. 30 (2009) 56–60.

[35] C. Gok, S. Aytas, Biosorption of uranium (VI) from aqueous solution using calcium alginate beads, J. Hazard. Mater. 168 (2009) 369–375.

[36] S.K. Papageorgiou, F.K. Katsaros, E.P. Kouvelos, J.W. Nolan, H. Le Deit, N.K. Kanellopoulos, Heavy metal sorption by calcium alginate beads from *Laminaria digitata*, J. Hazard. Mater. B137 (2006) 1765–1772.

[37] A.F. Hassan, A.M. Abdel-Mohsen, M.G. Fouda, Comparative study of calcium alginate, activated carbon, and their composite beads on methylene blue adsorption, Carbohydr. Polym. 102 (2014) 192–198.

[38] L. Liu, Y. Wan, Y. Xie, R. Zhai, B. Zhang, J. Liu, The removal of dye from aqueous solution using alginate-halloysite nanotube beads, Chem. Eng. J. 187 (2012) 210–216.

[39] A.N. Bezbaruah, S. Krajangpan, B.J. Chisholm, E. Khan, J.J. Elorza Bermudez, Entrapment of iron nanoparticles in calcium alginate beads for groundwater remediation applications, J. Hazard. Mater. 166 (2009) 1339–1343.

[40] D.E. Shahwar, A. Yasar, S. Yousaf, Solar assisted photo Fenton for cost effective degradation of textile effluents in comparison to AOPs, Global Nest J. 14 (2012) 477–486.

[41] B.S. Al-Tawabini, Treatment of water contaminated with Di-N-butyl phthalate by photo-Fenton process, Global Nest: Int. J. 5 (2003) 23–28.

[42] L. Xu, J. Wang, Degradation of 4-chloro-3,5-dimethylphenol by a heterogeneous Fenton-like reaction using nanoscale zero-valent iron catalysts, Environ. Eng. Sci. 30 (2013) 294–301.

[43] R. Karale, B. Manu, S. Shrihari, Degradation of toxic 2-aminopyridine pharmaceutical compound from aqueous environments using advanced Fenton and photo-Fenton oxidation processes, Int. J. Adv. Technol. Civil Eng. 2 (2013) 34–38.

[44] H. Abdul Aziz, M.M. Noor, A. Omran, Chemical oxidation of treated textile effluent by hydrogen peroxide and Fenton process, Environ. Eng. Manage. J. 9 (2010) 351–360.

[45] H.C. Shin, S.H. Park, H.G. Ahn, M. Chung, B.W. Kim, S.J. Kim, S.G. Seo, S.C. Jung, The effect of microwave-assisted for photo-catalytic degradation of rhodamine B in aqueous nano TiO_2 particles dispersions, J. Nanosci. Nanotechnol. 11 (2011) 1597–1600.

[46] H. Xu, M. Prasad, Y. Liu, A novel catalyst in mineral-catalyzed Fenton-like system for dyeing wastewater discoloration, J. Hazard. Mater. 165 (2009) 1186–1192.

[47] M. Argun, M. Karatas, S. Dursun, Treatment of mineral-oil recovery industry wastewater by sequential aeration and Fenton's oxidation process, Environ. Eng. Manage. J. 9 (2010) 643–649.

[48] J. Sun, S. Sun, M. Fan, H. Guo, L. Qiao, R. Sun, A kinetic study on the degradation of p-nitroaniline by Fenton oxidation process, J. Hazard. Mater. 148 (2007) 172–177.

[49] J.X. Chen, L.Z. Zhu, Heterogeneous UV–Fenton catalytic degradation of dyestuff in water with hydroxyl-Fe pillared bentonite, Catal. Today 126 (2007) 463–470.

[50] S. JianHui, F. JingLan, S. ShaoHui, P. YunQing, S. MengKe, S. Yan, Degradation of the antibiotic sulfamonomethoxine sodium in aqueous solution by photo-Fenton oxidation, Environ. Sci. Technol. 57 (2012) 558–564.

[51] H.A.A. Medien, S.M.E. Khalil, Kinetics of the oxidative decolorization of some organic dyes utilizing Fenton-like reaction in water, J. King Saud Univ. Sci. 22 (2010) 147–153.

[52] S. Hashemian, M. Tabatabaee, M. Gafari, Fenton oxidation of methyl violet in aqueous solution, J. Chem. 2013 (2013) 1–6.

[53] C.S. Chiou, C.F. Chang, C.Y. Chang, Y.P.Y.P. Wu, C.T. Chang, Y.S. Li, Y.H. Chen, Mineralization of polyethylene glycol in aqueous solution by hydrogen peroxide with basic oxygen furnace slag, Environ. Technol. 25 (2004) 1357–1365.

[54] Standard Methods for the Examination of Water and Wastewater, nineteenth ed., Supplement, "5310 Total Organic Carbon", American Public Health Association, Washington, DC, 1996, pp. 9–14.